Original Article

JCBFM

Journal of Cerebral Blood Flow & Metabolism
0(00) 1–10

DOI: 10.1177/0271678X16673385
jcbfm.sagepub.com

SAGE

Magnetic resonance imaging of blood–brain barrier permeability in ischemic stroke using diffusion-weighted arterial spin labeling in rats

Yash V Tiwari[1,2], Jianfei Lu[1,3], Qiang Shen[1], Bianca Cerqueira[1,2] and Timothy Q Duong[1]

Abstract

Diffusion-weighted arterial spin labeling magnetic resonance imaging has recently been proposed to quantify the rate of water exchange (K_w) across the blood–brain barrier in humans. This study aimed to evaluate the blood–brain barrier disruption in transient (60 min) ischemic stroke using K_w magnetic resonance imaging with cross-validation by dynamic contrast-enhanced magnetic resonance imaging and Evans blue histology in the same rats. The major findings were: (i) at 90 min after stroke (30 min after reperfusion), group K_w magnetic resonance imaging data showed no significant blood–brain barrier permeability changes, although a few animals showed slightly abnormal K_w. Dynamic contrast-enhanced magnetic resonance imaging confirmed this finding in the same animals. (ii) At two days after stroke, K_w magnetic resonance imaging revealed significant blood–brain barrier disruption. Regions with abnormal K_w showed substantial overlap with regions of hyperintense T_2 (vasogenic edema) and hyperperfusion. Dynamic contrast-enhanced magnetic resonance imaging and Evans blue histology confirmed these findings in the same animals. The K_w values in the normal contralesional hemisphere and the ipsilesional ischemic core two days after stroke were: 363 ± 17 and $261 \pm 18\,min^{-1}$, respectively ($P < 0.05$, $n = 9$). K_w magnetic resonance imaging is sensitive to blood–brain barrier permeability changes in stroke, consistent with dynamic contrast-enhanced magnetic resonance imaging and Evans blue extravasation. K_w magnetic resonance imaging offers advantages over existing techniques because contrast agent is not needed and repeated measurements can be made for longitudinal monitoring or averaging.

Keywords

Cerebral ischemia, hyperperfusion, vasogenic edema, Evans blue, dynamic contrast-enhanced magnetic resonance imaging, perfusion imaging, arterial spin labeling, rats

Received 22 April 2016; Revised 2 September 2016; Accepted 13 September 2016

Introduction

Stroke is a leading cause of death and long-term disability.[1] Recombinant tissue plasminogen activator (rtPA), the only food and drug administration-approved treatment for ischemic stroke, is effective in improving stroke outcomes, but unfortunately, rtPA benefits only 3–5% of stroke patients in the United States due to serious risk of hemorrhagic transformation and limited treatment window (within 3 h of stroke onset in the United States and 4.5 h in Europe of stroke onset).[2] Early disruption of the blood–brain barrier (BBB) integrity is a leading risk factor for rtPA-related cerebral hemorrhages.[3,4] In animal studies,

[1]Research Imaging Institute, University of Texas Health Science Center, San Antonio, TX, USA
[2]Department of Biomedical Engineering, University of Texas at San Antonio, TX, USA
[3]Department of Anatomy and Embryology, School of Basic Medical Sciences, Peking University Health Science Center, Beijing, China

Corresponding author:
Timothy Q Duong, Research Imaging Institute, University of Texas Health Science Center at San Antonio, 8403 Floyd Curl Dr, San Antonio, TX 78229, USA.
Email: timothy.duongmri@gmail.com

acute BBB impairment based on dynamic contrast-enhanced (DCE) magnetic resonance imaging (MRI) have been demonstrated to be a good predictor of symptomatic hemorrhagic transformation after rtPA treatment.[4] Increased BBB permeability has also been associated with spontaneous intracerebral hemorrhages.[5] In agreement with these findings, acute BBB impairment seen as early enhancement on DCE MRI after rtPA treatment has been linked to symptomatic intracranial hemorrhage in stroke patients.[6,7] Monitoring risk of hemorrhagic transformation after rtPA treatment remains challenging. Therefore, the ability to reliably image early disruption of BBB integrity (before symptomatic intracranial hemorrhage or significant compromise of BBB) and the ability to monitor BBB integrity after rtPA treatment could improve the safety of rtPA treatment (i.e. by excluding patients for rtPA treatment) and benefit more stroke patients. Moreover, knowledge of the BBB permeability could also guide drug delivery to the brain (i.e. timing drug delivery when BBB is disrupted).

In vivo imaging of BBB integrity remains challenging. Computed tomography is used clinically to rule out symptomatic hemorrhage, but cannot detect early disruption of BBB before symptomatic intracranial hemorrhage.[8] Thus, a negative finding could still post-risk of hemorrhagic transformation because impaired BBB may not be detectable on computed tomography. Positron emission tomography measures uptake of radioisotope labeled ligands as an index of BBB leakage.[9] Positron emission tomography is not widely available in hyperacute stroke management. Both computed tomography and positron emission tomography involve ionizing radiation.[10] DCE MRI to derive K^{Trans}, which provides an index of an exogenous contrast agent leakage from blood, has been utilized for imaging BBB permeability.[7,11–16] The need for an exogenous contrast agent could have significant negative side effects (i.e. nephrogenic systemic fibrosis and renal complications) and prevents repeated measurements to improve sensitivity, spatial resolution, and/or longitudinal monitoring of BBB integrity,[13] thereby limiting its widespread clinical utility for imaging BBB integrity in stroke.

A new MRI method based on diffusion-weighted arterial spin labeling (DW-ASL) technique has recently been proposed to quantify the rate of water exchange (K_w) across the BBB.[17,18] This technique uses diffusion weighting to differentiate magnetically tagged water (ASL) signal from the capillary and tissue compartments. The rate of water exchange K_w between the capillary and tissue compartment can be derived using a two-compartment model of the ASL signal. BBB dysfunction has been reported in brain tumors[17] and obstructive sleep apnea[19] using K_w MRI. Considering the size difference between water molecules and contrast agents, the water exchange rate has the potential to be more sensitive than K^{Trans} MRI. K_w MRI is non-invasive and thus repeated measurements can be made for longitudinal monitoring or averaging to augment sensitivity and spatial resolution. Our laboratory has recently cross-validated the K_w MRI technique against K^{Trans} MRI and Evans blue (EB) histology in the same animals in association with mannitol-induced disruption of the BBB.[20]

The goal of this study was to evaluate the feasibility of K_w MRI to detect BBB disruption in experimental ischemic stroke and compare this approach using K^{Trans} MRI and EB in the same animals.

Methods

Animal preparation

The manuscript is written in accordance to the ARRIVE guidelines. Experimental procedures were approved by the Institutional Animal Care and Use Committees of the University of Texas Health Science Center San Antonio, Texas and followed the National Institutes of Health's Guidelines for the Use and Care of Laboratory Animals (8th edition). Animals arrived to our facility at least five days before experimentation. Twelve healthy male Sprague-Dawley rats (250–300 g, 8–10 weeks old, Charles River Laboratories) were studied. Paired housing was used before stroke, and single housing was used after stroke in a Tecniplast caging system with autoclaved Sani-chip bedding. Lighting was set at 12-h light and 12-h dark cycle. The rats had ad libitum access to irradiated rodent chow from Harlan laboratories and autoclaved water. The justification of sample sizes was based on expected variances and differences between groups.

The experimental design is shown in Figure 1. Animals were mechanically ventilated (Model 683, Harvard Apparatus, South Natick, MA) under 1.5% isoflurane anesthesia in air during surgery. Tail vein was catheterized using PE-50 tubing for contrast agent delivery. Focal cerebral ischemia[21] of the right hemisphere was induced by middle cerebral artery occlusion (MCAO) using intraluminal filament (0.35–0.37 mm intraluminal silicon rubber-coated filaments, Doccol Corporation, Sharon, MA) inserted via the external carotid artery. The animal was secured in supine position using an MRI compatible rat stereotaxic headset and maintained at 1.2% isoflurane during MRI scans. End-tidal CO_2, rectal temperature, heart rate and arterial oxygenation saturation were recorded and maintained within normal physiological range during MRI experiments.

At 30 min after stroke, apparent diffusion coefficient (ADC) and cerebral blood flow (CBF) MRI were

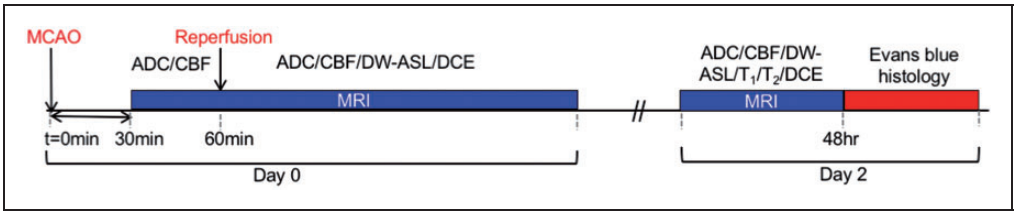

Figure 1. Experimental protocol of MCAO, reperfusion, MRI and EB measurement performed on rats.

measured to confirm the presence of a stroke and to delineate the perfusion–diffusion mismatch. Reperfusion was performed 60 min after occlusion, achieved by taking the animal out of the scanner to withdraw the filament occluder.[22] At 75 min, ADC and CBF were acquired to confirm successful reperfusion. At 90 min, DW-ASL MRI was acquired using two b values, followed by DCE MRI via a bolus of Gadolinium (Gd) contrast agent (0.2 ml/kg, Gadovist™, Bayer Health Care) through the tail vein, during which the dynamic scans continued. After the last MRI on day 0, animals recovered from anesthesia and returned to home cage.

At two days after stroke, T_2, ADC, CBF, DW-ASL, and DCE MRI were acquired. In addition, DW-ASL MRI was performed at multiple post-labeling delay (PLD) = 150, 250, 350, and 500 ms to evaluate effects of arterial transit time (ATT) on A_2 and K_w measurements. Additionally, T_1 maps were acquired on a subset of animal groups (n = 7). At the end of the MRI experiments, EB dye was injected through tail vein. About 2 h of circulation time after EB administration, the animals were euthanized for histological analysis.

MRI experiments

MRI experiments were performed on a 7 Tesla Bruker Biospec scanner with a 40 G/cm BGA12S gradient insert (Billerica, MA). Custom-made brain and neck surface coils were used for brain imaging and arterial spin labeling (ASL), respectively.[21,22]

ADC was measured using spin-echo diffusion-weighting gradients with spin-echo echo planar readout. The diffusion gradients were applied separately along the x, y, and z directions (three data sets to be averaged). Two b values of 0 and 1200 s/mm^2 were used. CBF measurements were performed using two-coil continuous ASL technique with gradient echo-planar readout. The continuous ASL sequence used a 2.7 ms square labeling RF pulse. T_2 maps were acquired using fast spin echo with four effective echo times (TE) (25, 40, 75, and 120 ms), echo train length = 8, and 4 signal averages. Other MRI scan parameters included: 4 slices, slice thickness = 3.0 mm, single-shot echo-planar imaging, matrix size = 96 × 96 (reconstructed to 128 × 128), field of view = 2.56 × 2.56 cm^2, flip angle = 90°, repetition time (TR) = 3 s, TE = 10.2 ms for CBF, and 30 ms for ADC measurements.[23]

T_1 maps were generated using six single-shot, inversion-recovery gradient-echo, echo-planar imaging. T_1-weighted images were acquired with inversion delay times = 0.025, 0.5, 1, 2, 4, 8 s, TR = 12 s, and NA = 4.[24]

DW-ASL MRI used continuous ASL followed by spin-echo diffusion-weighting module with echo-planar readout.[17,20] Diffusion weighting was applied in the z direction. MRI parameters were four 3.0-mm thick slices, FOV = 2.56 × 2.56 cm^2, matrix = 64 × 64 (reconstructed to 128 × 128), TR = 3000 ms, TE = 28 ms, δ = 1.6 ms, Δ = 7.08 ms, 60 averages, yielding a temporal resolution per one b value at one PLD of 6 min. DW-ASL was acquired using two b values (b = 0, 50 s/mm^2) at a single PLD of 400 ms. Additionally, DW-ASL was acquired at PLD = 150, 250, 350, and 500 ms at 48 h with b = 25 s/mm^2 to measure transit time changes.

DCE MRI (20 min) was acquired using a 2D multi-slice FLASH sequence.[15] First, a pre-scan module was used to determine the flip angle and M_0 distribution, which included three FLASH scans at different TRs: 54.41, 200 and 3000 ms.[15] The other imaging parameters were: four 3.0-mm coronal slices, TE = 2.408 ms, FOV = 2.56 × 2.56 cm^2, matrix = 128 × 128, and 30° nominal flip angle. Dynamic scans during Gd injection used the same parameters except TR of 54.41 ms, which yielded a temporal resolution of 6.6 s per image volume, and 90 time points were acquired.

EB

At 48 h after the last MRI, EB (4% solution, 4 ml/kg, Sigma-Aldrich, St. Louis, MO) was injected intravenously via the tail vein after the last MRI. About 2 h after EB injection while still under anesthesia, the brain was perfused with phosphate-buffered saline (0.01 M, 100 ml, Fisher Scientific) via the aorta to clear EB from bloodstream. The brain was then removed and sectioned with 3-mm thick slices to carefully match the MR images. The EB stained slices were then scanned and digitized.

Data analysis

Based on the two-compartment model of ASL signals, the capillary $\Delta M_c(t)$ and tissue $\Delta M_b(t)$ compartment of the ASL signals can be separated by their differences in ADCs.[17,18,20] DW-ASL signals can be characterized by biexponential decay

$$\Delta M(t, b)/\Delta M(t, 0) = A_1(t)\, e^{-bD_1} + A_2(t)\, e^{-bD_2} \quad (1)$$

where A_1 and A_2 are the fractions of the fast (vascular) and slow (tissue) components, respectively ($A_1 + A_2 = 1$), and D_1 and D_2 are the corresponding ADCs. A_2 is dependent on PLD and ATT for the labeled water to reach capillaries.

A_2 can be obtained by biexponential fitting of the DW-ASL data. Alternatively, as done in our study, A_2 map can be determined using two b-value approximations, which shortened acquisition time. This is because D_1 and D_2 differ by a factor of 100.[20] We have previously found no significant difference in A_2 between 6 and 2 b values.[20] A b value of 50 s/mm^2 was selected, as it yielded a clear separation between the fast and slow decaying regions of the curve in the biexponential curve.

If ATT is known, K_w can be estimated from A_2 via a lookup table.[17–19] In our study, the A_2-K_w lookup table used T_1 of blood at 7 T = 2.212 s,[25] T_1 of brain tissue (gray matter) at 7T = 1.8 s,[26] PLD = 350 ms (PLD > ATT of 250 ms)[27] and labeling duration = 2.33 s. In this paper, we mostly presented A_2 data instead of K_w because K_w calculation required additional parameters, which might change in ischemic stroke.

ADC, CBF, T_1, and T_2 maps were calculated as described in Shen et al.[21] K^{Trans} was calculated from DCE-MRI images as described in Li et al.[15] A difference map was obtained by subtraction of pre- and post-mannitol T_1-weighted images ($DCE_{subtraction}$). ROI analysis was performed using Mango (version 3.8, University of Texas Health Science Center, San Antonio). On day 0, three tissue types (normal, perfusion–diffusion mismatch and ischemic core) were classified based on 30-min ADC deficit and CBF deficit using critical threshold values of ADC (0.53×10^{-3} mm^2/s) and CBF (0.35 ml/g/min).[23,28] Perfusion–diffusion mismatch (which approximates the ischemic penumbra) was defined as the difference between perfusion deficit and ADC defined core. ADC, CBF, A_2, K_w, $DCE_{subtraction}$, K^{Trans} values were tabulated for the core, mismatch, and normal ROIs. At day 0, three animals were excluded from analysis due to poor CBF data. At day 2, one animal was excluded from analysis due to poor CBF data. The total animals used for the key analysis were nine, including all measurements at all time points.

On day 2, two tissue types (infarcted and normal) were classified in which the mean T_2 value from the normal hemisphere plus two standard deviations were used as the threshold for defining the infarct tissue.[29] ADC, CBF, A_2, K_w, $DCE_{subtraction}$, T_1, T_2 values were tabulated for the core and normal ROIs, defined by T_2 threshold.

For evaluating possible differences in transit time at 48 h after stroke, $\Delta M/M$ values in the grey matter regions were analyzed a function of PLDs (= 150, 250, 350, and 500 ms).

Statistical analysis

One-way ANOVA with Tukey's post-hoc test was used for comparison between normal, mismatch, and core tissue ROI values on day 0. Two-tailed unpaired t-test was used for comparisons between normal and infarct tissue ROI values on day 2. A P value of 0.05 was taken to be statistically significant. All values are reported as mean ± SEM unless stated otherwise.

Results

Figure 2 shows the typical ADC and CBF maps at 30 min after stroke (during occlusion). A consistently larger perfusion deficit area compared to ADC deficit area was observed in all animals, indicative of the perfusion–diffusion mismatch. The normal, core, and mismatch pixels were defined based on initial ADC and CBF maps at 30 min. Reperfusion occurred at 60 min after stroke. Figure 2 also shows the ADC, CBF, A_2, $DCE_{subtraction}$, and K^{Trans} maps at 75–100 min after stroke. K_w MRI started 30 min after reperfusion, i.e. 90 min after stroke onset. Abnormal CBF and ADC volumes were reduced compared to the area of initial abnormal CBF and ADC at 30 min, indicative of successful reperfusion. A few animals showed slight contrasts on A_2, $DCE_{subtraction}$, K^{Trans} maps in the ipsilesional compared to the contralesional hemisphere. However, the group data showed no significant differences between the two hemispheres. A_2, K_w, K^{Trans}, and EB maps were in general agreement with each other.

Group results for day 0 after stroke are summarized in Figure 3. At 30 min after stroke, ADC values in the mismatch and core tissue were significantly lower than normal tissue as expected ($P < 0.05$, one-way ANOVA and Tukey's post hoc test). ADC values in the mismatch tissue were significantly higher than those in core tissue ($P < 0.05$). CBF values in the mismatch and core tissue were significantly lower than those in normal tissue ($P < 0.05$). After reperfusion, reversals of CBF and ADC were observed. Group-average A_2 values in core tissue and mismatch were not significantly different from that of normal tissue ($P > 0.05$).

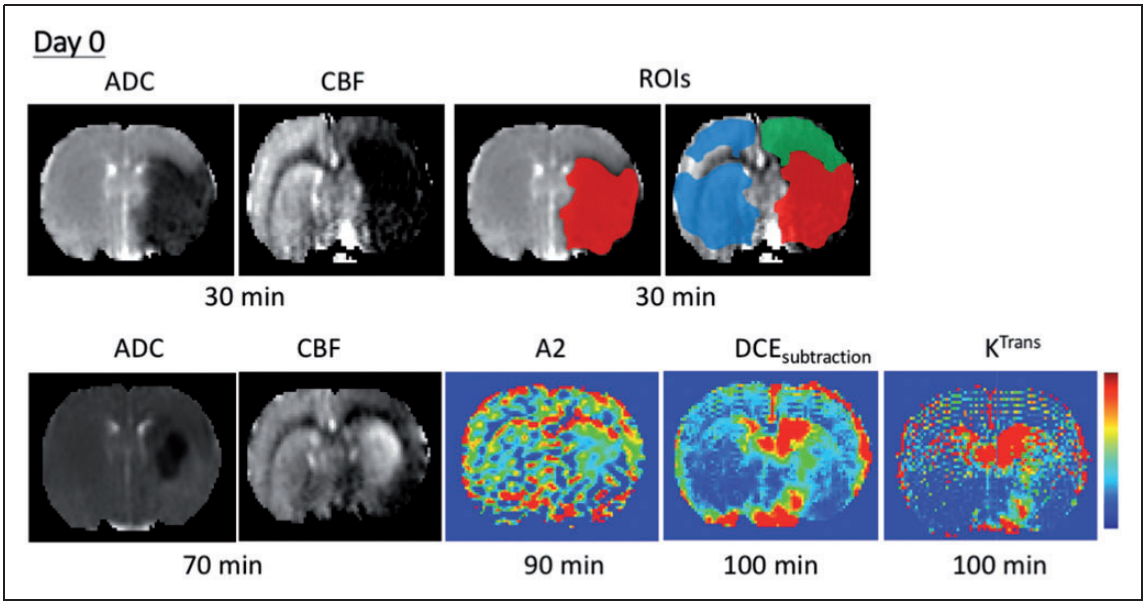

Figure 2. Typical ADC, CBF, A_2, $DCE_{subtraction}$ and K^{Trans} maps at day 0 after stroke (n = 9). Reperfusion was performed at 60 min after MCAO. ADC and CBF at 30 min after stroke during occlusion are also shown for reference, along with ROI definition for normal (blue), mismatch (green) and core (red). Scale bar: ADC (0–0.0001 s/mm^2), CBF (0–1.5 ml/g/min), A_2 (0.4–1.4), $DCE_{subtraction}$ (0–25,000 signal unit), K^{Trans} (0–0.003 min^{-1}).

Similarly, $DCE_{subtraction}$ values in the core and mismatch were also not significantly different from those in normal tissue ($P > 0.05$).

Figure 4 shows the typical T_2, ADC, CBF, T_1, A_2, $DCE_{subtraction}$, K^{Trans} maps, and EB histology two days after stroke. In the core tissue, T_2 and T_1 were elevated relative to those of normal tissue, indicative of vasogenic edema. ADC values in the ipsilesional hemisphere was slightly reduced but mostly pseudo-normalized. CBF values in the ipsilesional hemisphere were markedly elevated (hyperperfusion) above normal values. A_2 maps showed excellent contrast between infarct and normal tissue, indicating increased BBB permeability. Regions with lower A_2 substantially co-localized with regions of hyperintense T_2 and hyperperfusion. $DCE_{subtraction}$ and K^{Trans} maps also showed excellent contrast between infract and normal tissue. Increased EB extravasation was also observed, but its area of abnormality was smaller than area of abnormal A_2. A_2, K^{Trans}, and EB appeared overall similar in patterns but there were some distinct differences, namely: the area of abnormal EB was generally smaller than that of A_2, and K^{Trans}, and $DCE_{subtraction}$ showed very high signal changes in and around the lateral ventricle and areas with high vascular density at the base of the brain, in contrast to K_w (see Discussion section).

Group results for two days after stroke are summarized in Figure 5. T_2 and T_1 were significantly higher in infarct tissue compared to normal tissue, indicative of vasogenic edema ($P < 0.05$, unpaired two tailed t-test). ADC of infarct core, albeit lower, was not statistically different from normal tissue, indicative of pseudo-normalization. CBF of infarct tissue was significantly higher compared to normal tissue, indicative of hyperperfusion. A_2 of infarct tissue was significantly lower compared to normal tissue ($P < 0.05$), corroborated by increased $DCE_{subtraction}$ and K^{Trans} values ($P < 0.05$), indicative of BBB disruption.

In addition, ATT at 48 h after stroke was also evaluated, in which normalized ASL signals ($\Delta M/M$) were measured at different PLDs of 150, 250, 350, and 500 ms. We found no significant difference in normalized ASL signals between normal and infarct regions of 48 h after stroke for the range of PLDs ($P > 0.05$).

Discussion

This study evaluated BBB disruption in experimental ischemic stroke using K_w MRI and cross-validated this approach using K^{Trans} MRI and EB histology in the same animals. The major findings are: (i) at 90 min after stroke (30 min after reperfusion), K_w MRI shows no consistent BBB permeability changes, although a few animals showed slightly abnormal K_w. DCE MRI in the same animals confirms this finding. (ii) At two days after stroke, K_w MRI reveals significant disruption of BBB permeability. Regions with abnormal K_w show substantial overlap with regions of hyperintense T_2 (vasogenic edema) and hyperperfusion. K^{Trans} and EB histology in the same animals confirm this finding.

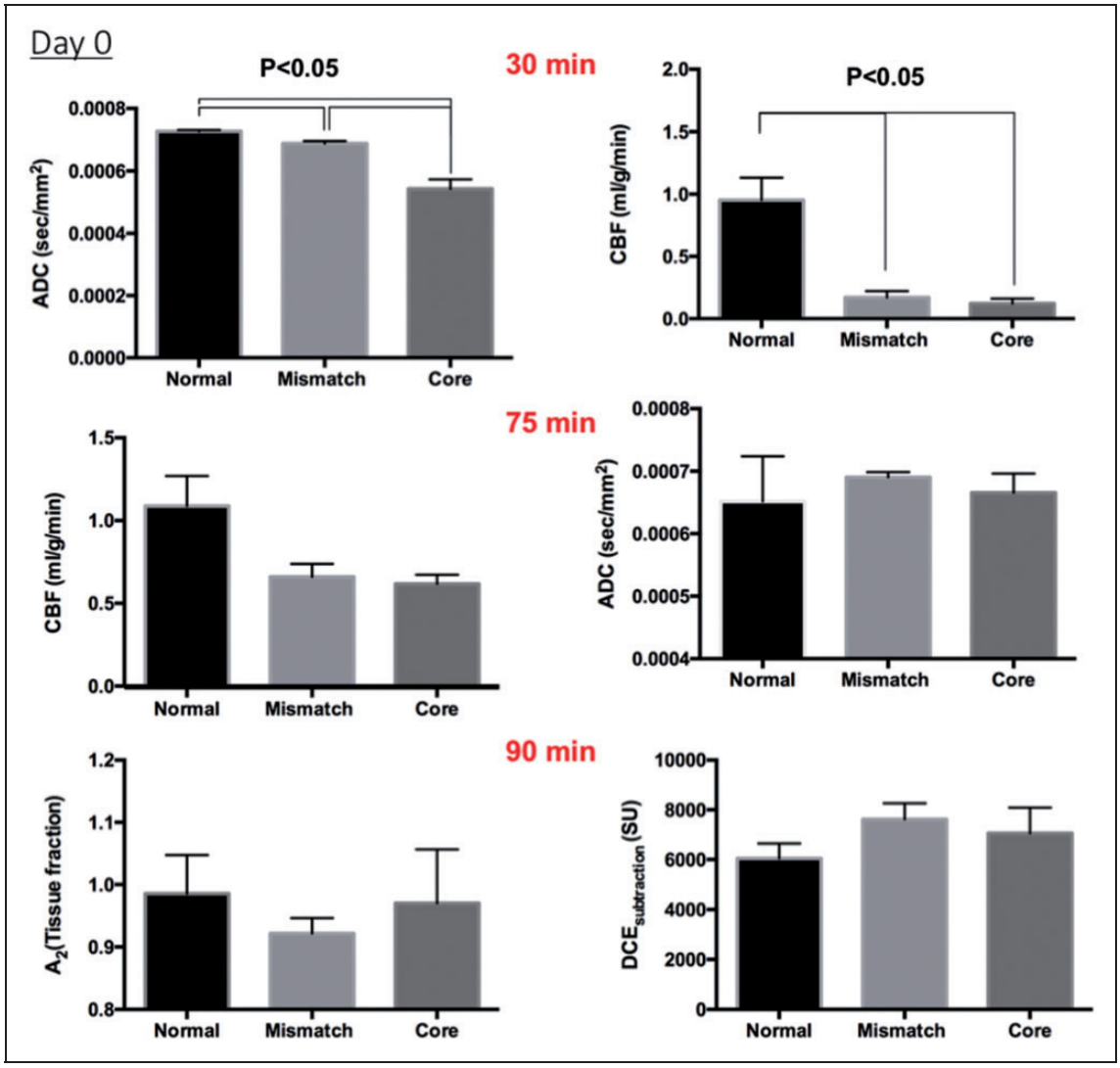

Figure 3. Group average values for ADC, CBF, $DCE_{subtraction}$ and A_2 in normal, mismatch and core tissue types at day 0. Error bars represent standard deviation around the mean values. ADC and CBF were acquired at 30 min after MCAO and 75 min after MCAO (after reperfusion). A_2 and DCE MRI were acquired at 90 min after MCAO, respectively.

Although the three maps show substantial overlaps, there are also some differences amongst the three maps. K_w values in the normal contralesional tissue and infarct ipsilesional tissue two days after stroke are 363 ± 17 and $261 \pm 18\,min^{-1}$, respectively. In conclusion, K_w MRI is sensitive to BBB permeability changes as a result of ischemic stroke, corroborated by K^{Trans} MRI and EB histology in the same animals.

ADC, CBF, T_2, and T_1 changes

ADC, CBF, T_2, and T_1 changes as well as lesion evolution and infarct volume in this study are consistent with our previously published MRI data on ischemic stroke,[21,23,30] including hyperperfusion at 48 h.[24,31]

Comparison with previous K_w MRI studies

The mean K_w of normal contralesional hemisphere in stroke animals was $363 \pm 17\,min^{-1}$ (48 h after stroke), higher than the value we reported previously ($252 \pm 38\,min^{-1}$) in normal rat brain.[20] This difference could be due to systemic differences between different animal groups, or stroke could affect K_w in the contralesional hemisphere. Although CBF in the normal hemisphere of stroke animals was slightly lower on day 2 but not on day 0 compared to normal animals, we do not believe this is major cause of the K_w differences between the two studies. Further investigation is needed. By comparison, K_w in human gray matter has been reported to be $193 \pm 50\,min^{-1}$,[17] $110 \pm 18\,min^{-1}$,[18]

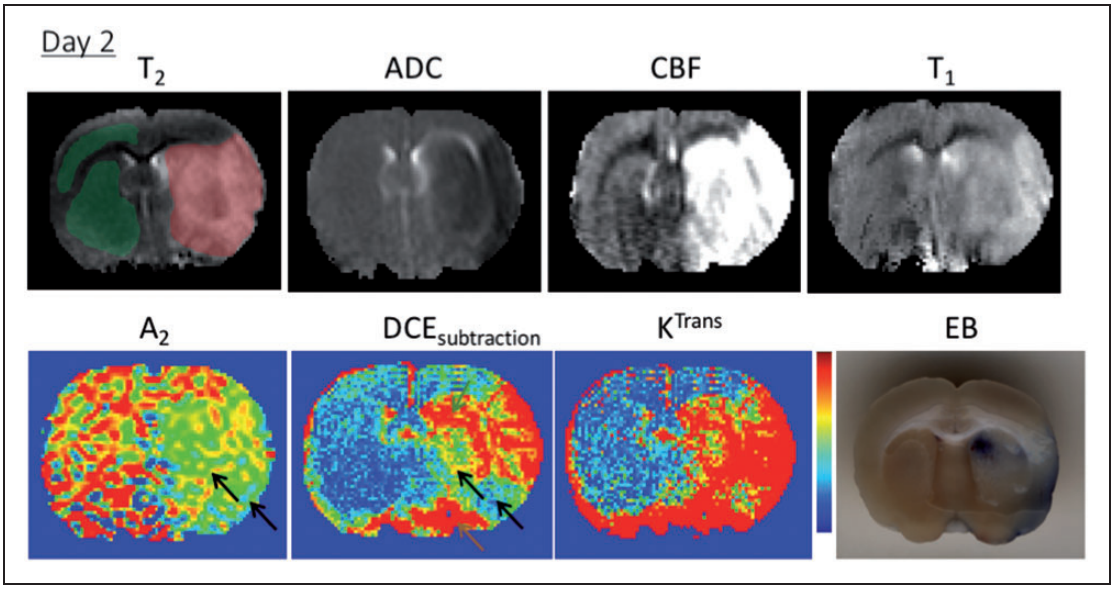

Figure 4. Typical T_2, ADC, CBF, T_1, A_2, $DCE_{subtraction}$, K^{Trans} maps and EB slices 2 days after stroke. The ROI definitions for normal (green) and infarcted tissue (red) are drawn on T_2 maps. Scale bar are: T_2 (40–120 ms), T_1 (1250–2500 ms), ADC (0–0.0001 s/mm^2), CBF (0–1.5 ml/g/min), A_2 (0.4–1.4), $DCE_{subtraction}$ (0–25,000 signal unit), K^{Trans} (0–0.003 min^{-1}).

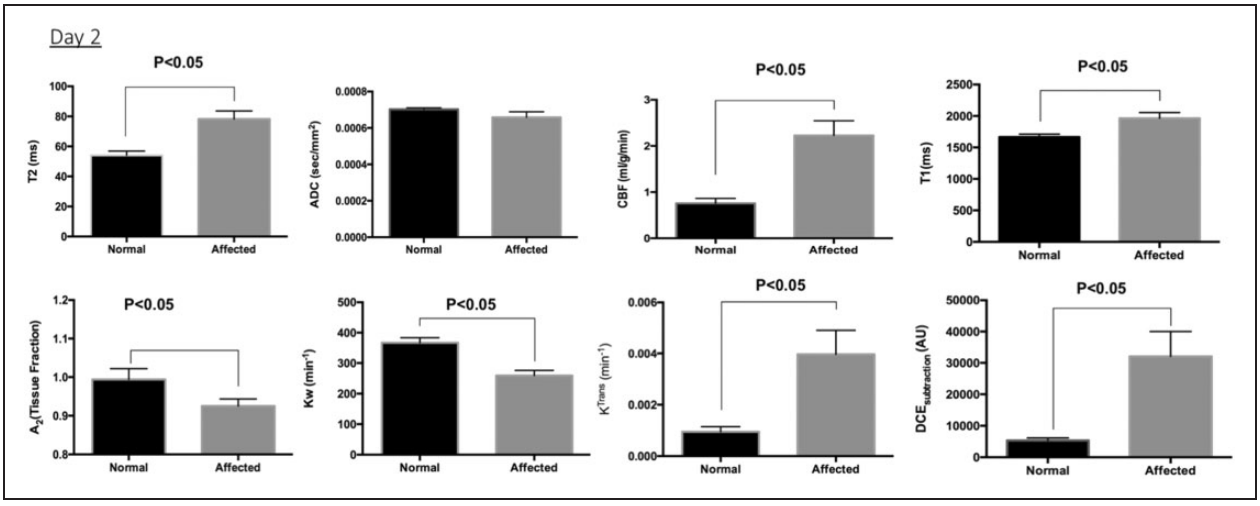

Figure 5. Group average values for T_2, ADC, CBF, T_1, A_2, $DCE_{subtraction}$ and K^{Trans} for normal and infracted tissue 2 days after MCAO. Error bars represent standard deviation around the mean values.

and $220.8 \pm 40.6\,min^{-1}$.[19] Our K_w values in rats are generally higher than those in humans. A possible explanation is that it could be due to species differences. Another possible explanation is that it could be due to the use of isoflurane in our animal study. It is also possible that K_w differs due to differences in MRI measurement and model parameters (see discussion section below).

K_w MRI has recently been cross-validated, in which mannitol was used to disrupt BBB in rats.[20] K_w MRI was found to be sensitive to mannitol-induced disruption of BBB permeability, and the extent of BBB disruption was mannitol dose dependent. A_2 and K_w decreased following mannitol-induced BBB disruption, consistent with stroke-induced BBB disruption in this study. Similarly, A_2 and K_w also decreased in patients with obstructive sleep apnea.[19]

A_2 changes after stroke

At 90 min after stroke (30 min after reperfusion), there were no significant A_2 changes in group data, although a few animals showed some slightly abnormal A_2, indicating overall no statistically significant changes in BBB

permeability at this time point. This is confirmed by DCE MRI. A likely explanation is that 60-min MCAO was not sufficiently severe and/or 30 min after reperfusion was not sufficiently long to cause significant and consistent BBB disruption. The literature works on BBB disruption immediately after reperfusion are sparse. While some studies have found BBB disruption as early as 2 h[32] and 3–5 h after stroke,[33] most reported BBB changes occurred only after several hours to days after stroke.[24,32–35]

At 48 h after stroke, there were substantial widespread changes in A_2 in the ischemic core, indicating marked BBB disruption, in general agreement with published literature where BBB disruption has been widely reported one to two days after stroke in rats.[24,32–35] Regions of A_2 abnormality overlapped substantially with regions of abnormal T_2 and hyperperfusion at 48 h, consistent with the notion that disrupted BBB permeability leads to hyperperfusion and hyperintense T_2. The marked increase in BBB permeability (detected by K_w and DCE MRI) and vasogenic edema (detected by T_2 MRI) is likely associated with the dysregulation of aquaporin channels, which has been linked to disruption of water transport following cerebral ischemia.[36,37]

Other factors that affect A_2 and K_w

While A_2 changes likely reflect increased BBB permeability, stroke affects a number of biophysical and physiological parameters that could alter A_2 and/or K_w. These parameters include T_1, T_2, ADC, transit time, CBF, and cerebral blood volume (CBV), amongst others, as discussed below.

ADC typically decreases 30–50% in acute ischemic stroke, pseudo-normalized, and increased in chronic stroke. This change could affect the results of DW-ASL biexponential fitting. However, D_1 and D_2 differ by two orders of magnitude (a factor of 100),[20] and thus the small D_2 changes due to ischemia per se is unlikely to significantly affect the results of DW-ASL biexponential fitting. This is consistent with the notion that at 90 min after stroke, A_2 remained normal whereas ADC decreased due to ischemia, suggesting A_2 is not affected by the relatively small ADC differences due to ischemia.

Transit time could increase after stroke. However, we found transit times were not significantly different between normal and abnormal tissue after reperfusion, suggesting that transit time did not significantly affect A_2 in our studies. Although transit time was not measured at 3 h due to time constraint, ATT is unlikely to be very different between normal and abnormal tissue because CBF had mostly returned to normal. During occlusion, A_2 and K_w are affected by transit time differences, but there is no need to measure BBB permeability in occluded vessels. Nonetheless, we predict that A_2 and K_w will markedly decrease in the ischemic territory where CBF is markedly reduced, providing contrast. Experiments are needed to verify this hypothesis. Transit time effect could be reduced by using a longer PLD or it can be taken into account in the modeling of A_2 and K_w. Transit time is less of an issue for small animals (as opposed to humans) and high fields because small animals have short ATTs ($\sim$250 ms in rats[27]) and high fields have longer T_1.

CBF and CBV could change after stroke. Changes in CBV after stroke could directly affect A_2 as the biexponential fitting is dependent on blood volume fraction. Such effect will need to be taken into account in the modeling of A_2 and K_w.

T_2 and T_1 could change after stroke, typically at least 6 h after stroke in rats and often with the advent of vasogenic edema. We do not expect T_2 to affect A_2 directly. T_1 changes affect CBF quantitation as well as the K_w modeling. Thus, such effects will need to be taken into account in the modeling of A_2 and K_w. Further studies are needed to evaluate the effects of T_2 and T_1 on A_2 and K_w

In sum, while A_2 and/or K_w are sensitive to BBB disruption following stroke, stroke alters some biophysical and physiological parameters that could affect A_2 and K_w determination. At 90 min after stroke (30 min after reperfusion), A_2 was not significantly affected by substantial changes in some biophysical and physiological parameters, suggesting that model parameters did not significantly affect A_2 estimates and that A_2 indeed accurately reflects BBB permeability changes. However, further studies are needed to quantify potential effects of these and other biophysical and physiological parameters on K_w determination.

Differences amongst A_2, K^{Trans}, and EB results

There were differences in magnitude and locations of permeability changes amongst the three maps. First, the area of abnormal EB was generally smaller than that of A_2. A possible explanation is A_2 measures water exchange, which is likely on a continuous spectrum. By contrast, EB measures dye leakage accumulated over 2 h, which likely yields more discrete change. Some of the differences could also be attributed to the measurements of these three methods being made sequentially at slightly different time points. Considering the size difference between water molecules and Gd contrast agent or EB, the water exchange rate is likely more sensitive than methods that depend on larger tracers or contrast agents. For example, it is likely that water movement across the BBB is abnormal before BBB becomes leaky to a larger tracer. Second, K^{Trans}

and $DCE_{subtraction}$ showed very high signal changes around the lateral ventricle and areas with high vascular density at the base of the brain, in contrast to K_w. This is expected because the choroid plexus outlining the lateral ventricle is permeable to Gd and blood vessels have residual Gd. Despite these differences, the cross-comparison study herein provided data supporting the notion that non-invasive K_w MRI is sensitive to BBB permeability changes in ischemic stroke.

Limitations

Although A_2 is not an intrinsic parameter, it is a useful index of BBB permeability and does not require additional physiological and biophysical parameters needed to calculate K_w. This is relevant because stroke could affect these physiological and biophysical parameters. Future studies will need to be taken into account when determining K_w in stroke. While we compared the correspondence amongst the three methods, further studies are needed to quantify their contrast-to-noise ratios to determine which methods are the most sensitive in detecting BBB integrity in ischemic stroke. This study used male, healthy young adult rats. Future studies will need to use animals of both genders, aged animals, as well as animals with comorbidities.

Conclusions

This study evaluated BBB disruption in experimental ischemic stroke using K_w MRI and cross-validated this approach using K^{Trans} MRI and EB histology in the same animals. K_w MRI is sensitive to BBB permeability changes as a result of ischemic stroke, and regions with abnormal K_w at 48 h after stroke coincide with regions of vasogenic edema and hyperperfusion. Future studies will vigorously monitor BBB integrity longitudinally from 0 to 6 h after stroke, quantify the contrast-to-noise ratio of K_w MRI with respect K^{Trans} and evaluate whether abnormal K_w predicts hemorrhagic transformation in an embolic stroke model. K_w MRI can also be applied to study traumatic brain injury, multiple sclerosis and Alzheimer's disease, amongst others, where BBB is expected to be disrupted.

Funding

The author(s) disclosed receipt of the following financial support for the research, authorship, and/or publication of this article: This work was supported in part by NIH/NINDS (R01-NS45879).

Declaration of conflicting interests

The author(s) declared no potential conflicts of interest with respect to the research, authorship, and/or publication of this article.

Authors' contributions

YT and TD designed the study and developed the methodology; YT, JL and BC carried out the study; YT and QS performed analysis; YT and TD wrote the manuscript. All authors approved the version to be published.

References

1. Mozaffarian D, Benjamin EJ, Go AS, et al. Heart disease and stroke statistics–2016 update: a report from the American Heart Association. *Circulation* 2016; 133: e38–e360.
2. Adeoye O, Hornung R, Khatri P, et al. Recombinant tissue-type plasminogen activator use for ischemic stroke in the United States: a doubling of treatment rates over the course of 5 years. *Stroke* 2011; 42: 1952–1955.
3. Dijkhuizen RM, Asahi M, Wu O, et al. Rapid breakdown of microvascular barriers and subsequent hemorrhagic transformation after delayed recombinant tissue plasminogen activator treatment in a rat embolic stroke model. *Stroke* 2002; 33: 2100–2104.
4. Neumann-Haefelin C, Brinker G, Uhlenkuken U, et al. Prediction of hemorrhagic transformation after thrombolytic therapy of clot embolism: an MRI investigation in rat brain. *Stroke* 2002; 33: 1392–1398.
5. Lee JM, Zhai G, Liu Q, et al. Vascular permeability precedes spontaneous intracerebral hemorrhage in stroke-prone spontaneously hypertensive rats. *Stroke* 2007; 38: 3289–3291.
6. Kassner A, Roberts TP, Moran B, et al. Recombinant tissue plasminogen activator increases blood-brain barrier disruption in acute ischemic stroke: an MR imaging permeability study. *AJNR Am J Neuroradiol* 2009; 30: 1864–1869.
7. Kastrup A, Groschel K, Ringer TM, et al. Early disruption of the blood-brain barrier after thrombolytic therapy predicts hemorrhage in patients with acute stroke. *Stroke* 2008; 39: 2385–2387.
8. Aviv RI, d'Esterre CD, Murphy BD, et al. Hemorrhagic transformation of ischemic stroke: prediction with CT perfusion. *Radiology* 2009; 250: 867–877.
9. Saha GB, MacIntyre WJ and Go RT. Radiopharmaceuticals for brain imaging. *Semin Nucl Med* 1994; 24: 324–349.
10. Gillard JH, Waldman AD and Barker PB. *Clinical MR neuroimaging: Physiological and functional techniques*. Engelska: Cambridge University Press, 2009.
11. Ewing JR, Knight RA, Nagaraja TN, et al. Patlak plots of Gd-DTPA MRI data yield blood-brain transfer constants concordant with those of 14C-sucrose in areas of blood-brain opening. *Magn Reson Med* 2003; 50: 283–292.
12. Ding G, Jiang Q, Li L, et al. Detection of BBB disruption and hemorrhage by Gd-DTPA enhanced MRI after embolic stroke in rat. *Brain Res* 2006; 1114: 195–203.
13. Kassner A, Mandell DM and Mikulis DJ. Measuring permeability in acute ischemic stroke. *Neuroimaging Clin N Am* 2011; 21: 315–325, x–xi.

14. Heye AK, Culling RD, Valdes Hernandez Mdel C, et al. Assessment of blood-brain barrier disruption using dynamic contrast-enhanced MRI. A systematic review. *NeuroImage Clin* 2014; 6: 262–274.
15. Li W, Long JA, Watts LT, et al. A quantitative MRI method for imaging blood-brain barrier leakage in experimental traumatic brain injury. *PLoS One* 2014; 9: e114173.
16. Li W, Watts LT, Shen Q, et al. Spatiotemporal dynamics of blood-brain barrier permeability, cerebral blood flow, T2 and diffusion following mild traumatic brain injury. *NMR Biomed* 2015; 29: 896–903.
17. Wang J, Fernandez-Seara MA, Wang S, et al. When perfusion meets diffusion: in vivo measurement of water permeability in human brain. *J Cereb Blood Flow Metab* 2007; 27: 839–849.
18. St Lawrence KS, Owen D and Wang DJ. A two-stage approach for measuring vascular water exchange and arterial transit time by diffusion-weighted perfusion MRI. *Magn Reson Med* 2012; 67: 1275–1284.
19. Palomares JA, Tummala S, Wang DJ, et al. Water exchange across the blood-brain barrier in obstructive sleep apnea: an mri diffusion-weighted pseudo-continuous arterial spin labeling study. *J Neuroimaging* 2015; 25: 900–905.
20. Tiwari YV, Huang L, Shen Q, et al. Blood brain barrier permeability by diffusion-weighted arterial spin labeling MRI: a cross-validation study. *Magn Reson Mag* 2016 (in press).
21. Shen Q, Ren H, Cheng H, et al. Functional, perfusion and diffusion MRI of acute focal ischemic brain injury. *J Cereb Blood Flow and Metab* 2005; 25: 1265–1279.
22. Shen Q, Du F, Huang S, et al. Neuroprotective efficacy of methylene blue in ischemic stroke: an MRI study. *PLoS One* 2013; 8: e79833.
23. Shen Q, Meng X, Fisher M, et al. Pixel-by-pixel spatiotemporal progression of focal ischemia derived using quantitative perfusion and diffusion imaging. *J Cereb Blood Flow and Metab* 2003; 23: 1479–1488.
24. Shen Q, Du F, Huang S, et al. Spatiotemporal characteristics of postischemic hyperperfusion with respect to changes in T1, T2, diffusion, angiography, and blood-brain barrier permeability. *J Cereb Blood Flow Metab* 2011; 31: 2076–2085.
25. Dobre MC, Ugurbil K and Marjanska M. Determination of blood longitudinal relaxation time (T1) at high magnetic field strengths. *Magn Reson Imaging* 2007; 25: 733–735.
26. Muir ER, Watts LT, Tiwari YV, et al. Quantitative cerebral blood flow measurements using MRI. *Methods Mol Biol* 2014; 1135: 205–211.
27. Thomas DL, Lythgoe MF, van der Weerd L, et al. Regional variation of cerebral blood flow and arterial transit time in the normal and hypoperfused rat brain measured using continuous arterial spin labeling MRI. *J Cereb Blood Flow Metab* 2006; 26: 274–282.
28. Meng X, Fisher M, Shen Q, et al. Characterizing the diffusion/perfusion mismatch in experimental focal cerebral ischemia. *Ann Neurol* 2004; 55: 207–212.
29. Tiwari YV, Jiang Z, Sun Y, et al. Effects of stroke severity and treatment duration in normobaric hyperoxia treatment of ischemic stroke. *Brain Res* 2016; 1635: 121–129.
30. Shen Q, Fisher M, Sotak CH, et al. Effects of reperfusion on ADC and CBF pixel-by-pixel dynamics in stroke: characterizing tissue fates using quantitative diffusion and perfusion imaging. *J Cereb Blood Flow Metab* 2004; 24: 280–290.
31. Tanaka Y, Nagaoka T, Nair G, et al. Arterial spin labeling and dynamic susceptibility contrast CBF MRI in postischemic hyperperfusion, hypercapnia, and after mannitol injection. *J Cereb Blood Flow Metab* 2011; 31: 1403–1411.
32. Strbian D, Durukan A, Pitkonen M, et al. The blood-brain barrier is continuously open for several weeks following transient focal cerebral ischemia. *Neuroscience* 2008; 153: 175–181.
33. Belayev L, Busto R, Zhao W, et al. Quantitative evaluation of blood-brain barrier permeability following middle cerebral artery occlusion in rats. *Brain Res* 1996; 739: 88–96.
34. Durukan A, Marinkovic I, Strbian D, et al. Post-ischemic blood-brain barrier leakage in rats: one-week follow-up by MRI. *Brain Res* 2009; 1280: 158–165.
35. Abo-Ramadan U, Durukan A, Pitkonen M, et al. Post-ischemic leakiness of the blood–brain barrier: a quantitative and systematic assessment by Patlak plots. *Exp Neurol* 2009; 219: 328–333.
36. Badaut J, Fukuda AM, Jullienne A, et al. Aquaporin and brain diseases. *Biochim Biophys Acta* 2014; 1840: 1554–1565.
37. Vella J, Zammit C, Di Giovanni G, et al. The central role of aquaporins in the pathophysiology of ischemic stroke. *Front Cell Neurosci* 2015; 9: 108.